Achieving three-dimensional entanglement between two spatially separated atoms by using the quantum Zeno effect

Siping Liu,[1,2] Jiahua Li,[1,*] Rong Yu,[3] and Ying Wu[1]

[1]*Wuhan National Laboratory for Optoelectronics and School of Physics, Huazhong University of Science and Technology, Wuhan 430074, People's Republic of China*

[2]*School of Physics and Electronic Engineering, Hubei University of Arts and Science, Xiangyang 441053, People's Republic of China*

[3]*School of Science, Hubei Province Key Laboratory of Intelligent Robot, Wuhan Institute of Technology, Wuhan 430073, People's Republic of China*

(Received 7 April 2013; published 17 June 2013)

Based on the quantum Zeno effect [B. Misra and E. C. G. Sudarshan, J. Math. Phys. **18**, 756 (1977)], we propose a scheme to achieve three-dimensional (3D) entanglement between two distant five-level atoms. In our scheme, the two atoms are trapped individually in two spatially-separated double-mode cavities connected by an optical fiber. It is found that the effective quantum Zeno dynamics of the composite cavity-fiber-cavity coupled system gives rise to the deterministic creation of the 3D entangled state with high fidelity. Moreover, only one step operation is required to complete the generation of the 3D entangled state. The numerical simulations clearly show that the proposed scheme is robust against the deviation of the system parameters and insensitive to various decoherence factors, including atomic spontaneous emissions, cavity decays and fiber photon leakages. We justify our scheme by considering the experimental feasibility within the currently available technology.

DOI: 10.1103/PhysRevA.87.062316 PACS number(s): 03.67.Mn, 42.50.Pq, 42.81.Qb

I. INTRODUCTION

Quantum entanglement introduced in physics originally by Schrödinger [1] is one of the most interesting characteristics in quantum mechanics and plays an important role in many quantum information processes (QIP) [2–5]. Various different schemes have been put forward to prepare entangled states in a controlled way in numerous quantum systems [6–15]. In particular, cavity quantum electrodynamics (QED) system provides one of the most promising and qualified candidates because of its low decoherent rate [12] and offers an almost ideal platform to realize this strong-coupling regime even on experiments [16], which is beneficial to create the entanglement. In the context of cavity QED, the entangled states have been experimentally demonstrated in two-state systems [17,18].

In the last few decades, the high-dimensional entanglement has attracted a lot of attention since quantum key distribution and quantum cryptography based on qutrit systems is more secure than those based on qubit systems [19–21]. Besides, high-dimensional entanglement can enhance the violation of local realism [22]. Plenty of theoretical and experimental schemes have been devoted to the preparation of high-dimensional entangled states of atoms [23–29] and photons [30–33] by selective absorption and emission of photons, adiabatic passages, and dispersive interactions between the atoms and optical cavities, and so on. For example, based on selective photon emission and absorption, Zheng *et al.* [28] proposed a scheme to generate three-dimensional (3D) entanglement with two nitrogen-vacancy (NV) centers coupled strongly to a bimodal microsphere cavity. Chen *et al.* [29] presented a robust scheme to prepare 3D entangled state between a single atom and a Bose-Einstein condensate (BEC) via stimulated Raman adiabatic passage (STIRAP) technique. Their numerical simulation shows that the proposed scheme is good enough to demonstrate the creation of this entangled state with high fidelity. Mair *et al.* [30] reported controllable preparations of the high-dimensional photonic entangled states based on the spatial modes of the electromagnetic field carrying orbital angular momentum. It is clearly shown that their proposed schemes can be used to define an infinitely dimensional discrete Hilbert space. Subsequently, two cavity QED schemes were put forward for producing high-dimensional entangled states of atoms with a nonresonant optical cavity by means of cavity-assisted collisions [23] and an external strong classical driving laser field [24], respectively. Nevertheless, the collisions of the atoms were experienced in one nonresonant cavity, which requires high experimental techniques and has a limited application in practical QIP.

On the other hand, the quantum Zeno effect (QZE) introduced in quantum physics originally by Misra and Sudarshan [34] is one of the specific quantum effects and is usually understood as the hindrance of the dynamics out of the initial state due to frequent or continuous von Neumann measurements [35–38]. For possible applications, the system may evolve away from its initial state and remain in the so-called Zeno subspace [39,40] through frequent projections onto a multidimensional subspace. This evolution is called a quantum Zeno dynamics (QZD) [41]. In addition, the "continuous coupling" [42] can reformulate the QZE and achieve the same physical effects between the system and detector without making use of projection operators and nonunitary dynamics. The QZE may open a novel route to study the possibility of tailoring the interaction so as to obtain robust subspaces against decoherence, useful for practical applications in quantum computation, quantum communication, and QIP [43–48].

For the purpose of clarity, now we give a concise review of the QZE in terms of continuous coupling. Assume that the evolution of the total system is governed by a generic Hamiltonian of the type $H_K = H + K H_c$ [38]. Here H is the Hamiltonian of the quantum system under study, H_c is

*Author to whom correspondence should be addressed: huajia_li@163.com

regarded as an additional interaction Hamiltonian carrying out the measurement, and K is a coupling constant. Under the limit that $K \to \infty$, one can consider the limiting evolution operator $U(t) = \lim_{K\to\infty} \exp(iKH_c t)U_K(t)$. In this case, the above result can be reexpressed as the form $U(t) = \exp(-iH_Z t) = \exp(-i\sum_n P_n H P_n t)$, where P_n is the eigenprojection of H_c belonging to the eigenvalue λ_n. As a result, the overall system is dominated by the limiting evolution operator $U_K(t) \sim \exp[-i\sum_n (K\lambda_n P_n + P_n H P_n)t]$, which is the main result based by our present work.

In this paper, by means of the above-mentioned QZD, we put forward an alternative scheme for generating 3D entangled state for two five-level atoms trapped individually in two spatially separated double-mode cavities. Two cavities are connected by an optical fiber. Compared with previous protocols [25–27], first, the 3D entanglement with this composite cavity-fiber-cavity QED system can be established with only one-step operation, which is useful in real experiments because the scheme effectively reduces the number of operations for experimental implementation. Second, our numerical results show that the proposed scheme is robust against the deviation of the system parameters and insensitive to spontaneous emission of the excited state and dissipation of the fibers. Third, the cavity fields are not excited really and thus is insensitive to the decays of the cavities (or the photon leakage of the cavity) owing to the evolution of the system in the null-excitation subspace under quantum Zeno conditions. Additionally, our scheme loosens the requirement of strong cavity-fiber coupling. By discussing the experimental feasibility within the currently available technology, we believe that our scheme is a promising way to realize the 3D maximally atomic entangled state in this composite cavity-fiber-cavity QED system.

The paper is organized as follows. In Sec. II, we establish physical model under investigation and derive the effective Hamiltonian of the coupled system and the evolution equations of the state vector under quantum Zeno conditions. In Sec. III, we are devoted to illustrating the generation of 3D atomic entangled state. In Sec. IV, we explore in detail the influences of atomic spontaneous decay, photon leakage out of the cavities, and optical fiber on the generation of atomic entangled states. In Sec. V, we provide a possible experimental realization of our scheme. Finally, our main conclusions are summarized in Sec. VI.

II. MODEL AND EQUATION

As illustrated in Fig. 1, we consider a composite cavity-fiber-cavity QED system in which tripod-type and M-type five-level atoms are individually trapped in two frequency-degenerate but polarization-nondegenerate two-mode cavities (cavities 1 and 2) connected by an optical fiber. In the cavity 1, the transition $|g_0\rangle_1 \Leftrightarrow |e\rangle_1$ of the tripod-type atom with transition frequency ω_{eg_0} is driven by a classical laser field from free space with angular frequency ω_1 and Rabi frequency Ω_1. The transitions $|e\rangle_1 \Leftrightarrow |l\rangle_1$ and $|e\rangle_1 \Leftrightarrow |r\rangle_1$ of the tripod-type atom with the same transition frequencies $\omega_{el} = \omega_{er}$ are coupled to the cavity modes a_{1l} and a_{1r} (l and r denote the left and right circularly polarization) with degenerate frequencies $\omega_l^{c_1} = \omega_r^{c_1} = \omega^{c_1}$ and coupling strengths g_{1l}, g_{1r}. In the cavity 2, the transitions $|e_l\rangle_2 \Leftrightarrow |l\rangle_2$ and $|e_r\rangle_2 \Leftrightarrow |r\rangle_2$ of the M-type atom with the same transition frequencies $\omega_{e_l l} = \omega_{e_r r}$ are simultaneously driven by an external classical laser field with angular frequency ω_2 and Rabi frequencies Ω_{2l}, Ω_{2r}. The transitions $|e_l\rangle_2 \Leftrightarrow |g\rangle_2$ and $|e_r\rangle_2 \Leftrightarrow |g\rangle_2$ of the M-type atom with the same transition frequencies $\omega_{e_l g} = \omega_{e_r g}$ are coupled by the cavity modes a_{2l} and a_{2r} with degenerate frequencies $\omega_l^{c_2} = \omega_r^{c_2} = \omega^{c_2}$ and coupling strengths g_{2l}, g_{2r}. Δ_1, and Δ_2 are the single photon frequency detunings and satisfy the relationship $\omega_{eg_0} - \omega_1 = \omega_{ek} - \omega_k^{c_1} = \Delta_1$ and $\omega_{e_k k} - \omega_2 = \omega_{e_k g} - \omega_k^{c_2} = \Delta_2$ ($k = l,r$), respectively. It should be emphasized that, in the short fiber limit, $(2L\overline{v})/(2\pi c) \ll 1$, where L is the length of the fiber and $\overline{v}$ is the decay rate of the cavity field into a continuum of fiber modes [49], only the resonant mode of the fiber interacts with the cavity modes.

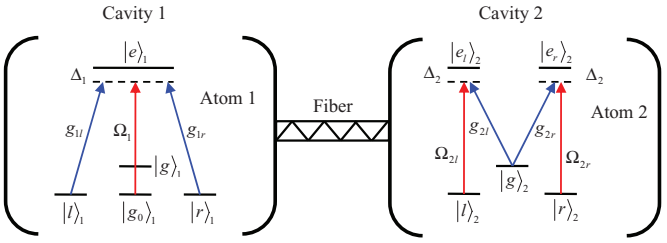

FIG. 1. (Color online) Schematic structure of optical composite system, which is composed of tripod-type and M-type five-level atoms, two frequency-degenerate but polarization-nondegenerate two-mode cavities, and an optical fiber. Tripod-type and M-type atoms (atom 1 and atom 2) are trapped in two spatially separated double-mode cavities 1 and 2, respectively. Two cavities are connected by an optical fiber.

Under the rotating-wave approximation (RWA), the resulting Hamiltonian describing the atom-cavity interaction can be written in the interaction picture as (setting $\hbar = 1$) [50,51]

$$H = H_1 + H_2, \tag{1}$$

$$H_1 = \Delta_1|e\rangle_1\langle e| + \Omega_1(|g_0\rangle_1\langle e| + |e\rangle_1\langle g_0|) + \sum_{k=l,r} x[\Delta_2|e_k\rangle_2\langle e_k| + (\Omega_{2k}|k\rangle_2\langle e_k| + \text{H.c.})], \tag{2}$$

$$H_2 = \sum_{k=l,r}(g_{1k}|e\rangle_1\langle k|a_{1k} + g_{2k}|e_k\rangle_2\langle g|a_{2k} + \text{H.c.}) + \sum_{k=l,r}[\eta_k b_k(a_{1k}^\dagger + a_{2k}^\dagger) + \text{H.c.}], \tag{3}$$

where the symbol H.c. means Hermitian conjugate. a_l, a_r and $a_l^\dagger$, $a_r^\dagger$ are the annihilation and creation operators associating with the corresponding quantized cavity modes. It should be pointed out that the last term in H_2 describes the interaction between the cavity modes and fiber modes with coupling strengths $\eta_k (k = l,r)$, where b_k and $b_k^\dagger$ are the annihilation and creation operators of the fiber modes. Ω_1, Ω_{2k}, g_{1k}, g_{2k}, and η_k are assumed to be real numbers and $\Omega_{2k} = \Omega_2$, $g_{1k} = g_1$, $g_{2k} = g_2$, and $\eta_k = \eta$, respectively.

For an initial state $|g_0\rangle_1|g\rangle_2|0_l0_r\rangle_{c_1}|0\rangle_f|0_l0_r\rangle_{c_2}$, the whole system evolution remains in the subspace spanned by

$$|1\rangle = |g_0\rangle_1|g\rangle_2|0_l0_r\rangle_{c_1}|0\rangle_f|0_l0_r\rangle_{c_2},$$
$$|2\rangle = |e\rangle_1|g\rangle_2|0_l0_r\rangle_{c_1}|0\rangle_f|0_l0_r\rangle_{c_2},$$

$$
\begin{aligned}
|3\rangle &= |l\rangle_1|g\rangle_2|1_l0_r\rangle_{c_1}|0\rangle_f|0_l0_r\rangle_{c_2},\\
|4\rangle &= |r\rangle_1|g\rangle_2|0_l1_r\rangle_{c_1}|0\rangle_f|0_l0_r\rangle_{c_2},\\
|5\rangle &= |l\rangle_1|g\rangle_2|0_l0_r\rangle_{c_1}|1_l\rangle_f|0_l0_r\rangle_{c_2},\\
|6\rangle &= |r\rangle_1|g\rangle_2|0_l0_r\rangle_{c_1}|1_r\rangle_f|0_l0_r\rangle_{c_2},\\
|7\rangle &= |l\rangle_1|g\rangle_2|0_l0_r\rangle_{c_1}|0\rangle_f|1_l0_r\rangle_{c_2},\\
|8\rangle &= |r\rangle_1|g\rangle_2|0_l0_r\rangle_{c_1}|0\rangle_f|0_l1_r\rangle_{c_2},\\
|9\rangle &= |l\rangle_1|e_l\rangle_2|0_l0_r\rangle_{c_1}|0\rangle_f|0_l0_r\rangle_{c_2},\\
|10\rangle &= |r\rangle_1|e_r\rangle_2|0_l0_r\rangle_{c_1}|0\rangle_f|0_l0_r\rangle_{c_2},\\
|11\rangle &= |l\rangle_1|l\rangle_2|0_l0_r\rangle_{c_1}|0\rangle_f|0_l0_r\rangle_{c_2},\\
|12\rangle &= |r\rangle_1|r\rangle_2|0_l0_r\rangle_{c_1}|0\rangle_f|0_l0_r\rangle_{c_2},
\end{aligned}
\tag{4}
$$

where in $|x\rangle_1|y\rangle_2|n_ln_r\rangle_{c_1}|q\rangle_f|m_lm_r\rangle_{c_2}$, $|x\rangle_1$ denotes the state of the tripod-type atom in the first cavity, $|y\rangle_2$ denotes the state of the M-type atom in the second cavity, $|n_ln_r\rangle_{c_1} \equiv |n_l\rangle_{c_1} \bigotimes |n_r\rangle_{c_1}$ denotes the Fock state in the two modes of the first cavity, $|k\rangle_f$ denotes the Fock state in the fiber mode, and $|m_lm_r\rangle_{c_2} \equiv |m_l\rangle_{c_2} \bigotimes |m_r\rangle_{c_2}$ denotes the Fock state in the two modes of the second cavity. n_l, n_r denote the photon numbers of the two modes for the first cavity, m_l, m_r denote the photon numbers of the two modes for the second cavity, and q denotes the photon numbers of the fiber modes.

Under the condition $\Delta_{1(2)}$, $\Omega_{1(2)} \ll \eta$, $g_{1(2)}$, the Hilbert subspace is split into nine invariant Zeno subspaces [38,41,47,48] as follows:

$$
\begin{aligned}
&H_{P_1} = \{|1\rangle,|11\rangle,|12\rangle,|\phi_1\rangle\}, \quad H_{P_2} = \{|\phi_2\rangle\}, \quad H_{P_3} = \{|\phi_3\rangle\},\\
&H_{P_4} = \{|\phi_4\rangle\}, \quad H_{P_5} = \{|\phi_5\rangle\}, \quad H_{P_6} = \{|\phi_6\rangle\},\\
&H_{P_7} = \{|\phi_7\rangle\}, \quad H_{P_8} = \{|\phi_8\rangle\}, \quad H_{P_9} = \{|\phi_9\rangle\},
\end{aligned}
\tag{5}
$$

where the corresponding eigenvalues are given by $\lambda_1 = 0$, $\lambda_2 = -a_1$, $\lambda_3 = a_1$, $\lambda_4 = -a_2$, $\lambda_5 = a_2$, $\lambda_6 = -b_1$, $\lambda_7 = b_1$, $\lambda_8 = -b_2$, and $\lambda_9 = b_2$ with the projection $P_i^\mu = |\mu\rangle\langle\mu|(|\mu\rangle \in H_{P_i})$. Here $a_1 = \sqrt{(2\eta^2 + g_2^2 - d_1)/2}$, $a_2 = \sqrt{(2\eta^2 + g_2^2 + d_1)/2}$, $b_1 = \sqrt{(2\eta^2 + 2g_1^2 + g_2^2 - d_2)/2}$, $b_2 = \sqrt{(2\eta^2 + 2g_1^2 + g_2^2 + d_2)/2}$, $d_1 = \sqrt{4\eta^4 + g_2^4}$, $d_2 = \sqrt{4\eta^4 + (2g_1^2 - g_2^2)^2}$, and

$$
\begin{aligned}
|\phi_1\rangle &= A_1\left(\frac{g_2}{g_1}|2\rangle - \frac{g_2}{\eta}|5\rangle - \frac{g_2}{\eta}|6\rangle + |9\rangle + |10\rangle\right),\\
|\phi_2\rangle &= A_2\left(-\varepsilon_1|3\rangle + \theta_1|4\rangle + \frac{\varepsilon_1 a_1}{\eta}|5\rangle + \chi_1|6\rangle + \frac{a_1}{g_2}|7\rangle - \frac{a_1}{g_2}|8\rangle - |9\rangle + |10\rangle\right),\\
|\phi_3\rangle &= A_3\left(\varepsilon_1|3\rangle - \theta_1|4\rangle + \frac{\varepsilon_1 a_1}{\eta}|5\rangle + \chi_1|6\rangle - \frac{a_1}{g_2}|7\rangle + \frac{a_1}{g_2}|8\rangle - |9\rangle + |10\rangle\right),\\
|\phi_4\rangle &= A_4\left(-\varepsilon_2|3\rangle - \theta_2|4\rangle - \frac{\varepsilon_2 a_2}{\eta}|5\rangle + \chi_2|6\rangle + \frac{a_2}{g_2}|7\rangle - \frac{a_2}{g_2}|8\rangle - |9\rangle + |10\rangle\right),\\
|\phi_5\rangle &= A_5\left(\varepsilon_2|3\rangle + \theta_2|4\rangle - \frac{\varepsilon_2 a_2}{\eta}|5\rangle + \chi_2|6\rangle - \frac{a_2}{g_2}|7\rangle + \frac{a_2}{g_2}|8\rangle - |9\rangle + |10\rangle\right),\\
|\phi_6\rangle &= A_6\left(\frac{2\delta_1 g_1}{b_1}|2\rangle - \delta_1|3\rangle - \delta_1|4\rangle - \xi_1|5\rangle + \zeta_1|6\rangle - \frac{b_1}{g_2}|7\rangle - \frac{b_1}{g_2}|8\rangle + |9\rangle + |10\rangle\right),\\
|\phi_7\rangle &= A_7\left(\frac{2\delta_1 g_1}{b_1}|2\rangle + \delta_1|3\rangle + \delta_1|4\rangle - \xi_1|5\rangle + \zeta_1|6\rangle + \frac{b_1}{g_2}|7\rangle + \frac{b_1}{g_2}|8\rangle + |9\rangle + |10\rangle\right),\\
|\phi_8\rangle &= A_8\left(\frac{2\delta_2 g_1}{b_1}|2\rangle - \delta_2|3\rangle - \delta_2|4\rangle + \xi_2|5\rangle + \zeta_2|6\rangle - \frac{b_2}{g_2}|7\rangle - \frac{b_2}{g_2}|8\rangle + |9\rangle + |10\rangle\right),\\
|\phi_9\rangle &= A_9\left(\frac{2\delta_2 g_1}{b_1}|2\rangle + \delta_2|3\rangle + \delta_2|4\rangle + \xi_2|5\rangle + \zeta_2|6\rangle + \frac{b_2}{g_2}|7\rangle + \frac{b_2}{g_2}|8\rangle + |9\rangle + |10\rangle\right),
\end{aligned}
\tag{6}
$$

with $\varepsilon_1 = \frac{(d_1-\eta^2)(d_1+g_2^2)-2\eta^4}{g_2a_1(d_1+g_2^2)}$, $\theta_1 = \frac{a_1(d_1+g_2^2)}{2\eta^2g_2}$, $\chi_1 = \frac{2\eta^2-g_2^2-d_1}{2\eta g_2}$, $\varepsilon_2 = \frac{(d_1+\eta^2)(d_1-g_2^2)-2\eta^4}{g_2a_2(d_1-g_2^2)}$, $\theta_2 = \frac{a_2(d_1-g_2^2)}{2\eta^2g_2}$, $\chi_2 = \frac{2\eta^2-g_2^2+d_1}{2\eta g_2}$, $\delta_1 = \frac{b_1(2g_1^2-g_2^2-d_2)}{2\eta^2g_2}$, $\xi_1 = \frac{(d_2-\eta^2)(2g_1^2-g_2^2-d_2)+2\eta^4}{\eta g_2(2g_1^2-g_2^2-d_2)}$, $\zeta_1 = \frac{b_1^2-g_2^2}{\eta g_2}$, $\delta_2 = \frac{b_2(2g_1^2-g_2^2+d_2)}{2\eta^2g_2}$, $\xi_2 = \frac{(d_2+\eta^2)(2g_1^2-g_2^2+d_2)-2\eta^4}{\eta g_2(2g_1^2-g_2^2+d_2)}$, $\zeta_2 = \frac{b_2^2-g_2^2}{\eta g_2}$, and $A_i (i = 1,2,\ldots,9)$ being the normalization factor for the eigenstate $|\phi_i\rangle$, respectively.

So the Hamiltonian of the system can be approximately written as [38]

$$
\begin{aligned}
H_{\rm app} &\cong \sum_{i,\mu,\nu}\left(\lambda_i P_i^\mu + P_i^\mu H_1 P_i^\nu\right)\\
&= \sum_i \lambda_i P_i + \sum_{i=2}^{9} 2A_i^2\Delta_2|\phi_i\rangle\langle\phi_i| + A_1^2(s^2\Delta_1 + 2\Delta_2)|\phi_1\rangle\langle\phi_1| + A_1\left[s\Omega_1|1\rangle\langle\phi_1| + \Omega_2\left(|11\rangle\langle\phi_1| + |12\rangle\langle\phi_1|\right) + \text{H.c.}\right].
\end{aligned}
\tag{7}
$$

If the initial state is $|\Psi(0)\rangle = |1\rangle = |g_0\rangle_1|g\rangle_2|0_l0_r\rangle_{c_1}|0\rangle_f|0_l0_r\rangle_{c_2}$, under the conditions $\Delta_{1(2)}$, $\Omega_{1(2)} \ll \eta$, $g_{1(2)}$, then $H_{\rm app}$ can be reduced to the form

$$H_{\rm eff} = A_1^2(s^2\Delta_1 + 2\Delta_2)|\phi_1\rangle\langle\phi_1| + A_1[s\Omega_1|1\rangle\langle\phi_1| + \Omega_2(|11\rangle\langle\phi_1| + |12\rangle\langle\phi_1|) + \text{H.c.}]. \tag{8}$$

After time t, the system state can be expressed as $|\Psi(t)\rangle = C_1|1\rangle + C_2|11\rangle + C_3|12\rangle + C_4|\phi_1\rangle$ and evolve in the domination of the Schrödinger equation

$$i\frac{\partial}{\partial t}|\Psi(t)\rangle = H_{\rm eff}|\Psi(t)\rangle. \tag{9}$$

Associating with Eqs. (8) and (9), we can obtain the analytical expressions of the coefficients C_i $(i = 1,\ldots,4)$, with the results

$$\begin{aligned}
C_1(t) &= \frac{1}{\beta(s^2+2\alpha^2)}\left\{2\alpha^2\beta + e^{-i\frac{A_1^2\overline{\Delta}}{2}t}s^2\left[\beta\cos\left(\frac{A_1\beta}{2}t\right) + iA_1\overline{\Delta}\sin\left(\frac{A_1\beta}{2}t\right)\right]\right\},\\
C_2(t) &= C_3(t) = \frac{s\alpha}{\beta(s^2+2\alpha^2)}\left\{\beta - e^{-i\frac{A_1^2\overline{\Delta}}{2}t}\left[\beta\cos\left(\frac{A_1\beta}{2}t\right) + iA_1\overline{\Delta}\sin\left(\frac{A_1\beta}{2}t\right)\right]\right\},\\
C_4(t) &= 2i\frac{s\Omega_1}{\beta}e^{-i\frac{A_1^2\overline{\Delta}}{2}t}\sin\left(\frac{A_1\beta}{2}t\right),
\end{aligned} \tag{10}$$

where $\overline{\Delta} = A_1^2(s^2\Delta_1 + 2\Delta_2)$, $g_2 = sg_1 = sg$, $\alpha = \Omega_2/\Omega_1$, and $\beta = \sqrt{A_1^2\overline{\Delta}^2 + 4\Omega_1^2(s^2+2\alpha^2)}$, respectively.

From the above equations, we notice that when $\frac{A_1\beta}{2}\tau = n\pi$, namely, $\tau = n\pi\frac{2}{A_1\beta}$ $(n = 1, 3, 5,\ldots)$ and $e^{-i\frac{A_1^2\overline{\Delta}}{2}\tau} = \frac{2\alpha^2}{s^2} = 1$, namely, $s = \sqrt{2}\alpha$ (corresponding to $C_2 = C_3 = \frac{1}{\sqrt{2}}$, $C_1 = C_4 = 0$), the system can evolve into the state $|\Psi(\tau)\rangle = \frac{1}{\sqrt{2}}(|11\rangle + |12\rangle) = \frac{1}{\sqrt{2}}(|l\rangle_1|l\rangle_2 + |r\rangle_1|r\rangle_2)|0_l0_r\rangle_{c_1}|0\rangle_f|0_l0_r\rangle_{c_2}$ if the initial state is $|\Psi(0)\rangle = |g_0\rangle_1|g\rangle_2|0_l0_r\rangle_{c_1}|0\rangle_f|0_l0_r\rangle_{c_2}$.

On the other hand, if the initial state is $|\Psi(0)\rangle = |g\rangle_1|g\rangle_2|0_l0_r\rangle_{c_1}|0\rangle_f|0_l0_r\rangle_{c_2}$, the system state remains unchanged during the process of evolution since it is a dark state of the Hamiltonian (1) with zero eigenvalue. To sum up, when the initial state is $|\Psi(0)\rangle = \frac{1}{\sqrt{3}}(\sqrt{2}|g_0\rangle_1|g\rangle_2|0_l0_r\rangle_{c_1}|0\rangle_f|0_l0_r\rangle_{c_2} + |g\rangle_1|g\rangle_2|0_l0_r\rangle_{c_1}|0\rangle_f|0_l0_r\rangle_{c_2})$, the system state evolves into the state $|\Psi(t)\rangle = \frac{1}{\sqrt{3}}(|l\rangle_1|l\rangle_2 + |r\rangle_1|r\rangle_2 + |g\rangle_1|g\rangle_2)|0_l0_r\rangle_{c_1}|0\rangle_f|0_l0_r\rangle_{c_2} = |\Psi_{3D}\rangle|0_l0_r\rangle_{c_1}|0\rangle_f|0_l0_r\rangle_{c_2}$ under appropriate conditions. As a result, one can obtain the 3D maximally entangled state of two spatially separated atoms in normal form $|\Psi_{3D}\rangle = \frac{1}{\sqrt{3}}(|l\rangle_1|l\rangle_2 + |r\rangle_1|r\rangle_2 + |g\rangle_1|g\rangle_2)$ which is completely separated from the cavity fields and the fiber modes.

III. GENERATION OF 3D ENTANGLEMENT BETWEEN TWO SPATIALLY SEPARATED FIVE-LEVEL ATOMS

In the above derivation, the 3D maximally entangled state $|\Psi_{3D}\rangle$ can be deterministically generated in an ideal situation, which includes $s = \sqrt{2}\alpha$ at a proper time. However, there are usually some deviations of the system parameters. To this end, we should consider the influence of this deviation on the fidelity F_{3D} of the 3D entangled state, which can be defined as $F_{3D} = |_{c_2}\langle 0_l0_r|_f\langle 0|_{c_1}\langle 0_r0_l|\langle\Psi_{3D}|\Psi(t)\rangle|^2$.

First of all, we consider the influence of the coupling strength η on the fidelity F_{3D} of the 3D entangled state. In Fig. 2, we find that the coupling strength η can not change the maximum value of the fidelity, but larger η means shorter operation time. For simplicity, we can chose the ratio $\eta/g = 1$ in the following discussion.

Next, we discuss the influence of two proportional coefficients s $(s = g_2/g_1)$ and α $(\alpha = \Omega_2/\Omega_1)$ on the fidelity F_{3D} of the 3D entangled state. In Fig. 3(a), we plot the fidelity F_{3D} of the 3D entangled state versus the dimensionless time parameter $\Omega_1 t$ for two different proportional coefficients of s. It is clearly shown from Fig. 3(a) that when the condition $s = \sqrt{2}\alpha$ is strictly satisfied, the 3D maximally entanglement of two atoms can be deterministically generated at proper time, which has nothing to do with the value of s. But smaller s means longer operation time, as can be seen from the analytical expressions of the coefficients $C_2(t)$ and $C_3(t)$ in Eq. (10). In Fig. 3(b), we plot the fidelity F_{3D} of the 3D entangled state as a function of proportional coefficient s. It is easy to see from Fig. 3(b), if $s \neq \sqrt{2}\alpha$, the fidelity F_{3D} is still higher than 98% with respect to the fluctuation of the parameter s from

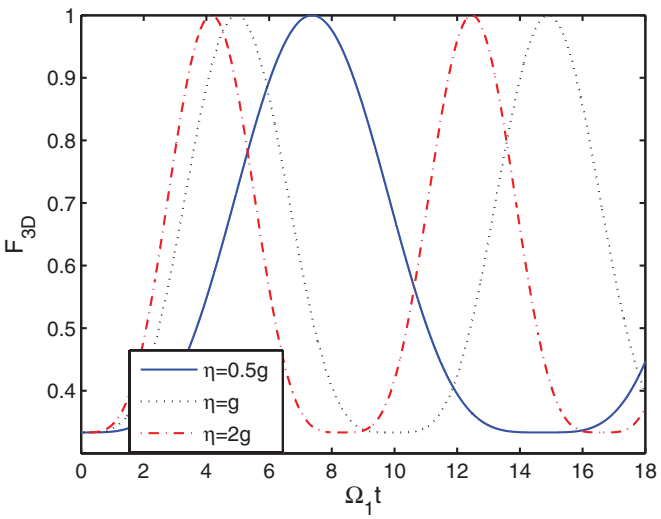

FIG. 2. (Color online) The fidelity F_{3D} of the 3D entangled state versus the dimensionless time parameter $\Omega_1 t$ for three different coupling strengths of η. Other system parameters are chosen as $\Delta_1 = \Delta_2 = 0$ and $s = \sqrt{2}\alpha$, respectively.

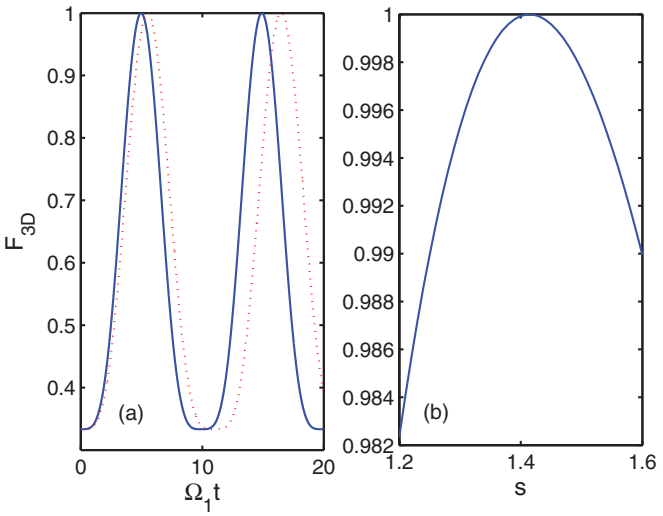

FIG. 3. (Color online) (a) The fidelity F_{3D} of the 3D entangled state versus the dimensionless time parameter $\Omega_1 t$ for two different proportional coefficients of s. The blue solid line denotes $s = 1$ and the red dashed line denotes $s = 0.8$, respectively; (b) The fidelity F_{3D} of the 3D entangled state as a function of proportional coefficient s. Other system parameters are chosen as (a) $\Delta_1 = \Delta_2 = 0$, $s = \sqrt{2}\alpha$; and (b) $\Delta_1 = \Delta_2 = 0$, $\alpha = 1$, $\Omega_1 t = 2\pi/(A_1\beta)$, respectively.

1.2 to 1.6. This suggests that the deviation of the proportional coefficient s has little influence on our results. On the other hand, we also plot the time evolution of the fidelity F_{3D} for three different proportional coefficients of α with $s = 1$ in Fig. 4. It is obviously indicated that the fidelity F_{3D} of the 3D entangled state can reach 96.79% even when α is fluctuated 20% around $1/\sqrt{2} \sim 0.707$. To summarize, the deviation of the proportional coefficients s and α around $s = \sqrt{2}\alpha$ has little influence on the generation of the 3D entangled state. In other words, our scheme is robust against the fluctuation of the proportional coefficients s and α.

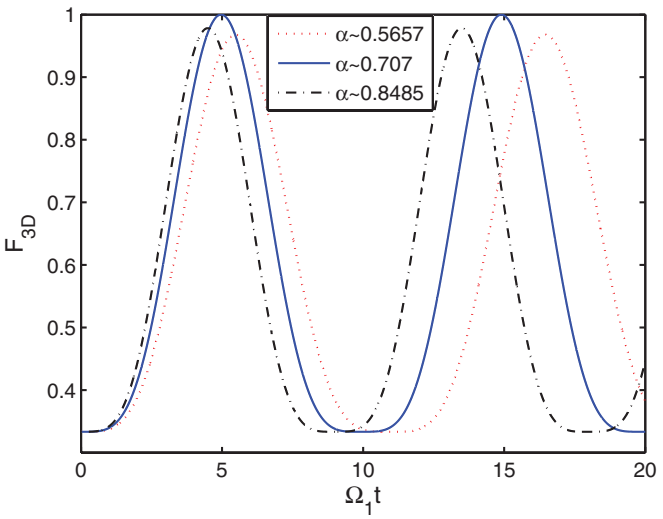

FIG. 4. (Color online) The fidelity F_{3D} of the 3D entangled state versus the dimensionless time parameter $\Omega_1 t$ for three different proportional coefficients of α. Other system parameters are chosen as $\Delta_1 = \Delta_2 = 0$ and $s = 1$, respectively.

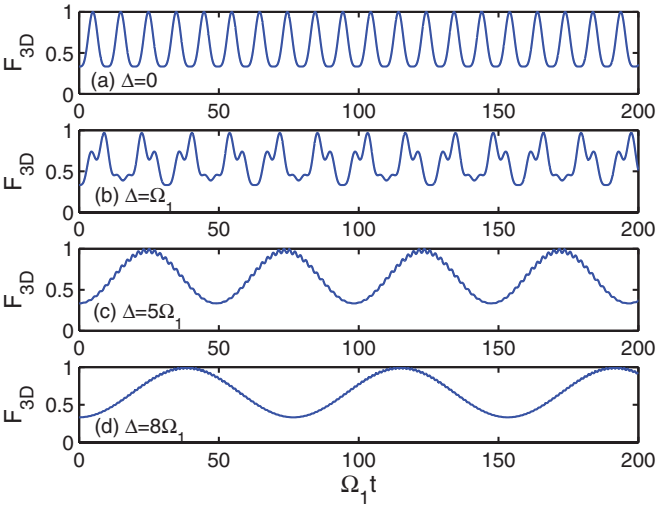

FIG. 5. (Color online) The fidelity F_{3D} of the 3D entangled state versus the dimensionless time parameter $\Omega_1 t$ for four different atom-cavity detunings of Δ. Other system parameters are chosen as $s = 1$ and $\alpha = 1/\sqrt{2}$, respectively.

Now, we consider the influence of the atom-cavity detunings Δ_1 and Δ_2 on the fidelity F_{3D} of the 3D entangled state. For convenience, we have assumed $\Delta_1 = \Delta_2 = \Delta$. The fidelity F_{3D} of the 3D entangled state between the two atoms as a function of the dimensionless time parameter $\Omega_1 t$ is plotted in Fig. 5 for four different detunings of Δ. It can been found from Fig. 5 that the 3D maximal entanglement of two atoms can be deterministically generated for different atom-cavity detunings under the condition $s = 1$ and $\alpha = 1/\sqrt{2}$, which is useful in real experiments. Furthermore, the operation time becomes longer with increasing the detunings Δ.

In the above discussion, the restriction $\Omega_{1(2)}$, $\Delta \ll g_{1(2)}$, which is called as the Zeno condition, is necessary. So we should consider the influence of the ratio $g_1/\Omega_1 = g/\Omega_1$ on the fidelity F_{3D} of the 3D entangled state. In Fig. 6, we plot the evolution of the fidelity F_{3D} versus the dimensionless time parameter $\Omega_1 t$ for three different ratios of g/Ω_1. It is easy to find that the maximum value of the fidelity F_{3D} is above 98% even when $g/\Omega_1 = 5$. We can get better behavior with larger g/Ω_1. In the following, we adopt the ratio $g/\Omega_1 = 10$.

There are a few assumptions and approximations in the derivation of the effective Hamiltonian. We should check the validity of these assumptions and the accuracy of our results. In Fig. 7, we plot the fidelity F_{3D} of the 3D entangled state as a function of the dimensionless time parameter $\Omega_1 t$ by directly solving the Schrödinger equation $i\frac{\partial}{\partial t}|\Psi(t)\rangle = H|\Psi(t)\rangle$ where H is original total Hamiltonian in Eq. (1) (see red dashed line in Fig. 7) and by using the effective Hamiltonian in Eq. (8) (see blue solid line in Fig. 7) based on QZE. We find that two curves agree with each other reasonably well, thus our effective model is valid.

IV. EFFECTS OF ATOMIC SPONTANEOUS DECAY AND PHOTON LEAKAGE OF THE CAVITIES AND FIBER

Until now, we ignored various decoherence effects including the spontaneous decay of the excited states of two

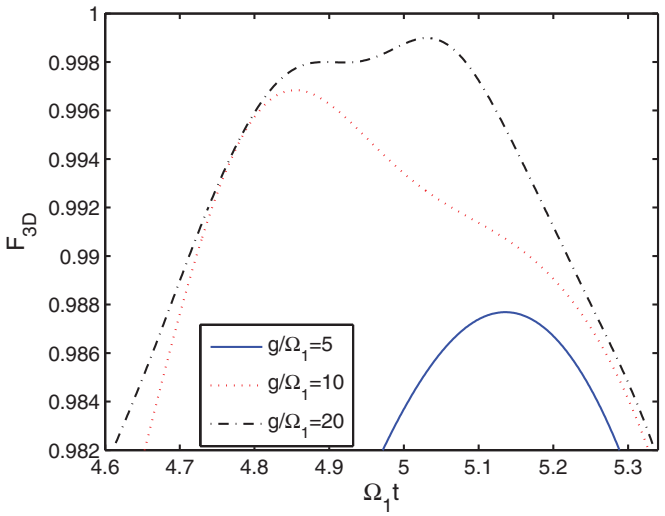

FIG. 6. (Color online) The fidelity F_{3D} of the 3D entangled state versus the dimensionless time parameter $\Omega_1 t$ for three different ratios of g/Ω_1. Other system parameters are chosen as $s = 1$, $\alpha = 1/\sqrt{2}$, and $\Delta = 0$, respectively.

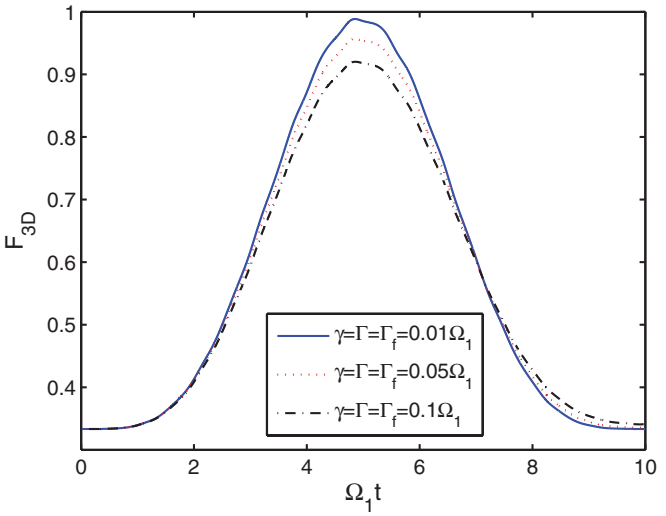

FIG. 8. (Color online) The fidelity F_{3D} of the 3D entangled state versus the dimensionless time parameter $\Omega_1 t$ for three different decay rates. Other system parameters are chosen as $s = 1$, $\alpha = 1/\sqrt{2}$, and $\Delta = 0$, respectively.

atoms and photon leakage out of the cavities and fiber. Experimentally, the spontaneous decay of the atoms is one of the major obstacles for generating 3D entanglement. In this section, we take into account the effect of the photon leakage and the excited state spontaneous emission of the two atoms. Using the density-matrix formalism, the master equation for the density matrix of the whole system can be written as

$$\dot{\rho}(t) = -i\,[H_{\text{total}}, \rho(t)] - \sum_{i=1,2}\sum_{k=l,r}\frac{\Gamma_{ik}}{2} \times (a_{ik}^{\dagger}a_{ik}\rho - 2a_{ik}\rho a_{ik}^{\dagger} + \rho a_{ik}^{\dagger}a_{ik})$$

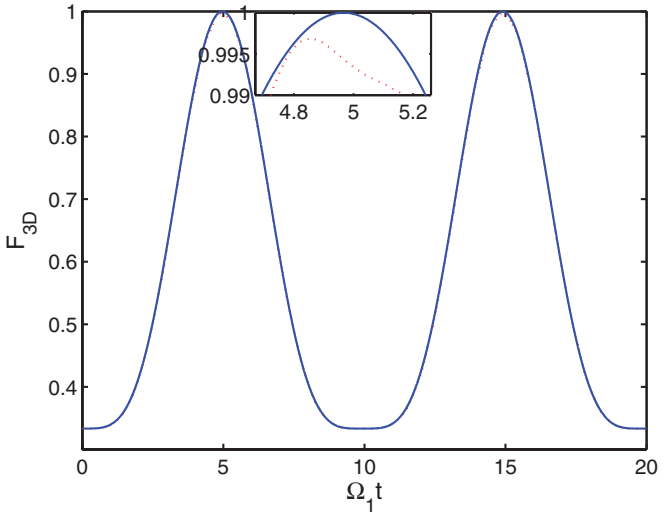

FIG. 7. (Color online) The fidelity F_{3D} of the 3D entangled state versus the dimensionless time parameter $\Omega_1 t$, calculated by using the total Hamiltonian (1) (red dashed line) and the effective Hamiltonian (8) under the Zeno condition (blue solid line). The system parameters are chosen as $g = 10\Omega_1$, $s = 1$, $\alpha = 1/\sqrt{2}$, and $\Delta = 0$, respectively.

$$- \sum_{k=l,r}\frac{\Gamma_{fk}}{2}(b_k^{\dagger}b_k\rho - 2b_k\rho b_k^{\dagger} + \rho b_k^{\dagger}b_k) - \sum_{i=1,2}\sum_{k=l,r}\frac{\gamma_{ik}}{2}(\sigma_{ik}^{+}\sigma_{ik}^{-}\rho + \rho\sigma_{ik}^{+}\sigma_{ik}^{-} - 2\sigma_{ik}^{-}\rho\sigma_{ik}^{+}), \tag{11}$$

where $\sigma_{1k}^{-} = |k\rangle_1\langle e|$ ($\sigma_{2k}^{-} = |k\rangle_2\langle e_k|$) is the atomic transition or projection operator between the states $|k\rangle_1$ ($|k\rangle_2$) and $|e\rangle_1$ ($|e_k\rangle_2$). Γ_{jk} and Γ_{fk} ($j = 1,2$; $k = l,r$) represent the cavity decay rate and the fiber decay rate, respectively. γ_{1k} denotes the spontaneous decay rate from $|e\rangle_1 \to |k\rangle_1$ of the first atom and γ_{2k} denotes the spontaneous decay rate from $|e_k\rangle_2 \to |k\rangle_2$ of the second atom. Without loss of generality, we set $\Gamma_{1k} = \Gamma_{2k} = \Gamma$, $\Gamma_{fk} = \Gamma_f$, and $\gamma_{1k} = \gamma_{2k} = \gamma$. From Fig. 8, we note that the maximum value of the fidelity F_{3D} can reach higher 98.9% for the case of $\gamma = \Gamma = \Gamma_f = 0.01\Omega_1$. Even for $\gamma = \Gamma = \Gamma_f = 0.1\Omega_1$ the maximum fidelity is also more than 92%.

In order to show the effect of γ, Γ, and Γ_f more clearly on the generation of the 3D entangled state, in Fig. 9 we plot the fidelity F_{3D} versus three different decay rates γ (blue solid line), Γ (red dashed line), and Γ_f (black dot-dashed line). It is clearly seen from Fig. 9 that the fidelity F_{3D} of the 3D entangled state is mainly affected by the spontaneous decay of atoms and almost unaffected by cavity decay owing to the evolution of the whole system in the subspace without excitation of the cavity mode fields. In short, our protocol is robust against the spontaneous decay and photon leakage.

V. POSSIBLE EXPERIMENTAL REALIZATION

Before ending this paper, let us briefly discuss the possible experimental realization of our proposed scheme of Fig. 1, which are given as follows.

(i) The level structure of the tripod-type and M-type atoms trapped in two spatially separated double-mode cavities 1 and 2 can be realized in cold alkali-metal atoms

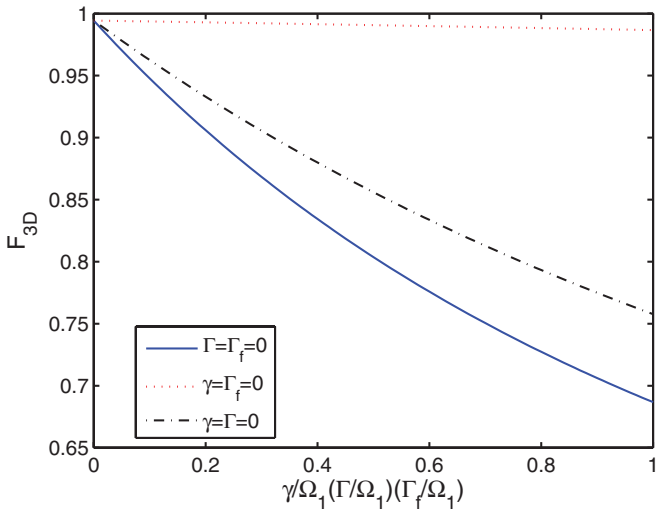

FIG. 9. (Color online) The fidelity F_{3D} of the 3D entangled state versus three different decay rates γ, Γ, and Γ_f when $\Omega_1 t = \sqrt{\frac{5}{2}}\pi$. Other system parameters are chosen as $s = 1, \alpha = 1/\sqrt{2}$, and $\Delta = 0$, respectively.

^{133}Cs (nuclear spin $I = 7/2$) using the $6S_{1/2} - 6P_{1/2}$ transition of D_1 line at 894.6 nm [26,52,53]. The designated states can be chosen as follows: $|g_0\rangle_1 = |6S_{1/2}, F = 3, m = 0\rangle$, $|g\rangle_1 = |6S_{1/2}, F = 4, m = 0\rangle$, $|l\rangle_1 = |6S_{1/2}, F = 3, m = +1\rangle$, $|r\rangle_1 = |6S_{1/2}, F = 3, m = -1\rangle$, and $|e\rangle_1 = |6P_{1/2}, F = 3, m = 0\rangle$ for the first atom in cavity 1 and $|l\rangle_2 = |6S_{1/2}, F = 3, m = +1\rangle$, $|r\rangle_2 = |6S_{1/2}, F = 3, m = -1\rangle$, $|g\rangle_2 = |6S_{1/2}, F = 4, m = 0\rangle$, $|e_l\rangle_2 = |6P_{1/2}, F = 4, m = +1\rangle$, and $|e_r\rangle_2 = |6P_{1/2}, F = 4, m = -1\rangle$ for the second atom in cavity 2, respectively. A zero-field splitting between lower sublevels $|6S_{1/2}, F = 3\rangle$ and $|6S_{1/2}, F = 4\rangle$ is ~9.2 GHz. A zero-field splitting between upper sublevels $|6P_{1/2}, F = 3\rangle$ and $|6P_{1/2}, F = 4\rangle$ is ~ 1.2 GHz The decay rates from excited to ground state, for the Cs D_1 line, $\gamma/2\pi = 4.6$ MHz, i.e., the natural linewidth of Cs D_1 line.

(ii) As shown in Ref. [54], a type of frequency-degenerate but polarization-nondegenerate two-mode cavity QED setup can be constructed experimentally. The cavity fields are coupled to the fiber with high efficiency [55,56]. The levels of atoms and polarizations of cavity modes and classical fields are shown in Fig. 10. Specifically, in Fig. 10(a), a π-polarized classical laser field, supplied by an external cavity diode laser (ECDL), is applied to drive the transition $|g_0\rangle_1 = |6S_{1/2}, F = 3, m = 0\rangle \Leftrightarrow |e\rangle_1 = |6P_{1/2}, F = 3, m = 0\rangle$. The transitions $|l\rangle_1 = |6S_{1/2}, F = 3, m = 1\rangle \Leftrightarrow |e\rangle_1 = |6P_{1/2}, F = 3, m = 0\rangle$ and $|r\rangle_1 = |6S_{1/2}, F = 3, m = -1\rangle \Leftrightarrow |e\rangle_1 = |6P_{1/2}, F = 3, m = 0\rangle$ are independently coupled to each of the orthogonally polarized cavity-1 modes with σ^- and σ^+ polarizations. In Fig. 10(b), another π-polarized classical laser field is applied to simultaneously couple the transitions $|l\rangle_2 = |6S_{1/2}, F = 3, m = +1\rangle \Leftrightarrow |e_l\rangle_2 = |6P_{1/2}, F = 4, m = +1\rangle$ and $|r\rangle_2 = |6S_{1/2}, F = 3, m = -1\rangle \Leftrightarrow |e_r\rangle_2 = |6P_{1/2}, F = 4, m = -1\rangle$. The transitions $|g\rangle_2 = |6S_{1/2}, F = 4, m = 0\rangle \Leftrightarrow |e_l\rangle_2 = |6P_{1/2}, F = 4, m = +1\rangle$ and $|g\rangle_2 = |6S_{1/2}, F = 4, m = 0\rangle \Leftrightarrow |e_r\rangle_2 = |6P_{1/2}, F = 4, m = -1\rangle$ are independently coupled to each of the cavity-2 fields with σ^+ and σ^- polarizations. Based on the recent experiments about realizing high-Q cavity and strong atom-cavity coupling [54,57–61], we can choose the experimental parameters as $g_{1(2)}/2\pi \sim 5.5$ GHz, $\Omega_1/2\pi \sim 0.55$ GHz, $\Omega_2/2\pi \sim 0.39$ GHz, $\gamma/2\pi \sim 4.6$ MHz, and $\Gamma/2\pi \sim 1.5$ MHz (corresponding to the cavity quality factor $Q \sim 10^8$). Under these achievements, we believe that the 3D entangled state of two atoms may be created with high fidelity based on our proposed scheme.

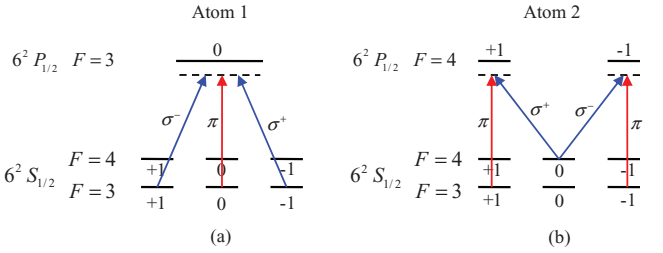

FIG. 10. (Color online) The energy levels of (a) atom 1 and (b) atom 2, and polarizations of double-cavity modes and external driven laser fields. π, σ^-, and σ^+ denote linearly, left-circularly, and right-circularly polarized components, respectively.

VI. CONCLUSION

In summary, by exploiting the QZE, we have proposed a protocol for creating 3D entanglement between two distant atoms trapped individually in two double-mode cavities, where two cavities are connected by an optical fiber. The results show that the 3D maximum entangled state with near-unity fidelity can be deterministically generated at proper time in ideal cases. In nonideal cases, the numerical simulations also indicate that the fidelity of generating the 3D entanglement is highly stable to the deviation of the system parameters from those in the ideal cases. Alternatively, it has been found that our scheme is robust against the photon leakage of the cavity and fiber and atomic spontaneous decay of the excited state because of the evolution of the whole system in a subspace without exciting the cavity field. Moreover, only one-step operation is required to complete the generation of the 3D entangled state. Finally, the experimental feasibility of our protocol is discussed by considering realistically achievable parameters. Therefore, we believe that the protocol proposed here is a promising avenue to realize the high-dimensional entanglement with present experimental techniques.

ACKNOWLEDGMENTS

Part of this work has been supported by the National Natural Science Foundation of China (NNSFC) (Grants No. 11004069, No. 11275074, and No. 91021011), by the Doctoral Foundation of the Ministry of Education of China (Grant No. 20100142120081), and by the National Basic Research Program of China (Contract No. 2012CB922103). We would like to thank Professor Xiaoxue Yang for her encouragement and helpful discussion.

[1] E. Schrödinger, Naturwissenschaften **23**, 807 (1935); **23**, 823 (1935); **23**, 844 (1935); [English translation by J. D. Trimmer, Proc. Am. Philos. Soc. **124**, 323 (1980)].

[2] M. A. Nielsen and I. L. Chuang, *Quantum Computation and Quantum Information* (Cambridge University Press, Cambridge, 2000).

[3] A. Barenco, Contemp. Phys. **37**, 375 (1996).

[4] L. Diósi, Lect. Notes Phys. **622**, 157 (2003).

[5] C. H. Bennett and D. P. Sicincenzo, Nature (London) **404**, 247 (2000).

[6] I. L. Chuang and Y. Yamamoto, Phys. Rev. A **52**, 3489 (1995).

[7] G. X. Li, H. T. Tan, and M. Macovei, Phys. Rev. A **76**, 053827 (2007).

[8] G. X. Li, S. S. Ke, and Z. Ficek, Phys. Rev. A **79**, 033827 (2009).

[9] P. Peng and F. L. Li, Phys. Rev. A **75**, 062320 (2007).

[10] X. B. Zou, K. Pahlke, and W. Mathis, Phys. Rev. A **68**, 024302 (2003).

[11] J. H. Reina, L. Quiroga, and N. F. Johnson, Phys. Rev. A **62**, 012305 (2000).

[12] T. Pellizzari, S. A. Gardiner, J. I. Cirac, and P. Zoller, Phys. Rev. Lett. **75**, 3788 (1995).

[13] Y. Wu, K. W. Chan, M. C. Chu, and P. T. Leung, Phys. Rev. A **59**, 1662 (1999).

[14] Q. A. Turchette, C. S. Wood, B. E. King, C. J. Myatt, D. Leibfried, W. M. Itano, C. Monroe, and D. J. Wineland, Phys. Rev. Lett. **81**, 3631 (1998).

[15] J. I. Cirac and P. Zoller, Phys. Rev. Lett. **74**, 4091 (1995).

[16] G. Khitrova, H. M. Gibbs, M. Kira, S. W. Koch, and A. Scherer, Nature Phys. **2**, 81 (2006).

[17] S. Osnaghi, P. Bertet, A. Auffeves, P. Maioli, M. Brune, J. M. Raimond, and S. Haroche, Phys. Rev. Lett. **87**, 037902 (2001).

[18] A. Rauschenbeutel, G. Nogues, S. Osnaghi, P. Bertet, M. Brune, J. M. Raimond, and S. Haroche, Science **288**, 2024 (2000).

[19] M. Bourennane, A. Karlsson, and G. Björk, Phys. Rev. A **64**, 012306 (2001).

[20] D. Bruß and C. Macchiavello, Phys. Rev. Lett. **88**, 127901 (2002).

[21] N. J. Cerf, M. Bourennane, A. Karlsson, and N. Gisin, Phys. Rev. Lett. **88**, 127902 (2002).

[22] D. Kaszlikowski, P. Gnacinski, M. Zukowski, W. Miklaszewski, and A. Zeilinger, Phys. Rev. Lett. **85**, 4418 (2000).

[23] X. B. Zou, K. Pahlke, and W. Mathis, Phys. Rev. A **67**, 044301 (2003).

[24] S. B. Zheng, Phys. Rev. A **68**, 035801 (2003).

[25] P. B. Li and F. L. Li, Opt. Express **19**, 1207 (2011).

[26] X. Y. Lü, J. B. Liu, C. L. Ding, and J. H. Li, Phys. Rev. A **78**, 032305 (2008).

[27] S. B. Zheng, Eur. Phys. J. D **54**, 719 (2009).

[28] A. S. Zheng, X. Y. Hao, and X. Y. Lü, J. Phys. B: At. Mol. Opt. Phys. **44**, 165507 (2011).

[29] L. B. Chen, P. Shi, C. H. Zheng, and Y. J. Gu, Opt. Express **20**, 14547 (2012).

[30] A. Mair, A. Vaziri, G. Weihs, and A. Zeilinger, Nature (London) **412**, 313 (2001).

[31] A. Lamas-Linares, J. C. Howell, and D. Bouwmeester, Nature (London) **412**, 887 (2001).

[32] J. C. Howell, A. Lamas-Linares, and D. Bouwmeester, Phys. Rev. Lett. **88**, 030401 (2002).

[33] A. Vaziri, G. Weihs, and A. Zeilinger, Phys. Rev. Lett. **89**, 240401 (2002).

[34] B. Misra and E. C. G. Sudarshan, J. Math. Phys. (NY) **18**, 756 (1977).

[35] C. B. Chiu, E. C. G. Sudarshan, and B. Misra, Phys. Rev. D **16**, 520 (1977).

[36] A. Peres, Amer. J. Phys. **48**, 931 (1980).

[37] W. M. Itano, D. J. Heinzen, J. J. Bollinger, and D. J. Wineland, Phys. Rev. A **41**, 2295 (1990).

[38] P. Facchi, G. Marmo, and S. Pascazio, J. Phys: Conf. Ser. **196**, 012017 (2009).

[39] P. Facchi, S. Pascazio, A. Scardicchio, and L. S. Schulman, Phys. Rev. A **65**, 012108 (2001).

[40] P. Facchi, V. Gorini, G. Marmo, S. Pascazio, and E. C. G. Sudarshan, Phys. Lett. A **275**, 12 (2000).

[41] P. Facchi and S. Pascazio, Phys. Rev. Lett. **89**, 080401 (2002).

[42] P. Facchi and S. Pascazio, in *Progress in Optics*, edited by E. Wolf (Elsevier, Amsterdam, 2001).

[43] A. Luis, Phys. Rev. A **63**, 052112 (2001).

[44] X. B. Wang, J. Q. You, and F. Nori, Phys. Rev. A **77**, 062339 (2008).

[45] A. Beige, D. Braun, B. Tregenna, and P. L. Knight, Phys. Rev. Lett. **85**, 1762 (2000).

[46] J. D. Franson, B. C. Jacobs, and T. B. Pittman, Phys. Rev. A **70**, 062302 (2004).

[47] W. A. Li and G. Y. Huang, Phys. Rev. A **83**, 022322 (2011).

[48] W. A. Li and L. F. Wei, Opt. Express **20**, 13440 (2012).

[49] A. Serafini, S. Mancini, and S. Bose, Phys. Rev. Lett. **96**, 010503 (2006).

[50] M. O. Scully and M. S. Zubairy, *Quantum Optics* (Cambridge University Press, Cambridge, 1997), Chap. 14, p. 409.

[51] Y. Wu, L. Wen, and Y. Zhu, Opt. Lett. **28**, 631 (2003).

[52] D. A. Steck, "Cesium D Line Data," available online at http://steck.us/alkalidata (revision 2.1.4, 23 December 2010).

[53] Y. Wu and X. Yang, Phys. Rev. A **70**, 053818 (2004).

[54] Y. Eto, A. Noguchi, P. Zhang, M. Ueda, and M. Kozuma, Phys. Rev. Lett. **106**, 160501 (2011).

[55] S. M. Spillane, T. J. Kippenberg, O. J. Painter, and K. J. Vahala, Phys. Rev. Lett. **91**, 043902 (2003).

[56] P. E. Barclay, K. Srinivasan, O. Painter, B. Lev, and H. Mabuchi, Appl. Phys. Lett. **89**, 131108 (2006).

[57] D. W. Vernooy, V. S. Ilchenko, H. Mabuchi, E. W. Streed, and H. J. Kimble, Opt. Lett. **23**, 247 (1998).

[58] S. M. Spillane, T. J. Kippenberg, K. J. Vahala, K. W. Goh, E. Wilcut, and H. J. Kimble, Phys. Rev. A **71**, 013817 (2005).

[59] W. L. Yang, Z. Y. Xu, M. Feng, and J. F. Du, New J. Phys. **12**, 113039 (2010).

[60] W. L. Yang, Z. Q. Yin, Z. Y. Xu, M. Feng, and J. F. Du, Appl. Phys. Lett. **96**, 241113 (2010).

[61] S. Zhang, X. Q. Shao, L. Chen, Y. F. Zhao, and K. H. Yeon, J. Phys. B: At. Mol. Opt. Phys. **44**, 075505 (2011).